U.S. National Library of Medicine
National Center for Biotechnology Information

NLM Citation: Cheng KT, Chakrabarti A, Aruva MR, et al. ^{99m}Tc-*N*,*N*′-Bis(*S*-benzoyl-thioglycoloyl)diamidopropanoyl-KRAS-PNA-D(Cys-Ser-Lys-Cys). 2007 Aug 9 [Updated 2008 Jan 3]. In: Molecular Imaging and Contrast Agent Database (MICAD) [Internet]. Bethesda (MD): National Center for Biotechnology Information (US); 2004-2013.
Bookshelf URL: https://www.ncbi.nlm.nih.gov/books/

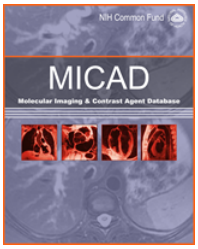

^{99m}Tc-*N*,*N*′-Bis(*S*-benzoyl-thioglycoloyl)diamidopropanoyl-KRAS-PNA-D(Cys-Ser-Lys-Cys)

^{99m}Tc-WT4351

Kenneth T. Cheng, PhD,[1] Atis Chakrabarti, PhD,[2] Mohan R. Aruva, PhD,[3] Mathew L. Thakur, PhD,[4] and Eric Wickstrom, PhD[5]

Created: August 9, 2007; Updated: January 3, 2008.

Chemical name:	^{99m}Tc-*N*,*N*′-Bis(*S*-benzoyl-thioglycoloyl)diamidopropanoyl)-KRAS-PNA-D(Cys-Ser-Lys-Cys)
Abbreviated name:	^{99m}Tc-WT4351
Synonym:	^{99m}Tc-KRAS PNA-peptide chimera, ^{99m}Tc-SBTG$_2$DAP-KRAS-PNA-D(CSKC)
Agent Category:	Peptide
Target:	IGF1 receptor (IGF1R), KRAS mRNA
Target Category:	Binding to IGF1R, internalized, and hybridized to KRAS mRNA
Method of detection:	Single-photon emission computed tomography (SPECT) and planar gamma imaging
Source of signal:	^{99m}Tc
Activation:	No

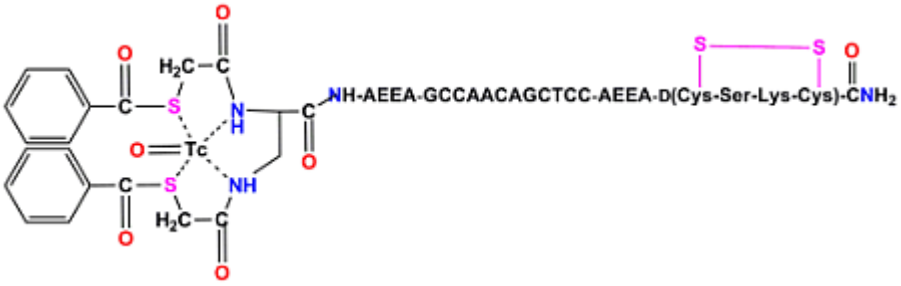

Author Affiliations: 1 National Center for Biotechnology Information, NLM, NIH, Bethesda, MD; Email: micad@ncbi.nlm.nih.gov. 2 Thomas Jefferson University, Philadelphia, PA; Email: atischakrabarti@yahoo.com. 3 Thomas Jefferson University, Philadelphia, PA; Email: Mohanr_aruva@yahoo.com. 4 Thomas Jefferson University, Philadelphia, PA; Email: Mathew.thakur@jefferson.edu. 5 Thomas Jefferson University, Philadelphia, PA, Corresponding Author; Email: eric@tesla.tju.edu.

Table continued from previous page.

Studies:	• *In vitro* • Rodents	^{99m}Tc-WT4351 structure. Tc represents ^{99m}Tc. The ^{99m}Tc coordination configuration has not been confirmed by experiments. Click on protein, nucleotide (RefSeq), and gene for more information about IGF1.

Background

[PubMed]

^{99m}Tc-*N*,*N*′-Bis(*S*-benzoyl-thioglycoloyl)diamidopropanoyl-KRAS-PNA-D(Cys-Ser-Lys-Cys) (^{99m}Tc-WT4351) is a ^{99m}Tc-peptide-PNA-peptide chimera that was developed as a gene expression agent for single-photon emission computed tomography (SPECT) imaging of pancreatic cancer (1, 2). ^{99m}Tc-WT4351 is designed to bind to the insulin-like growth factor 1 (IGF1) receptor and to internalize and hybridize with oncogene *KRAS* oncogene messenger RNA (mRNA) that is overexpressed in pancreatic cancer.

Pancreatic cancer is the fourth leading cause of cancer death in the United States (3). The ras gene family encodes a 21-kDa membrane-bound protein, Ras, involved in cell proliferation and migration, and the KRAS is typically activated by point mutations in codon 12 as a "signature" of pancreatic cancer (4). About 90% of patients with pancreatic cancer carry activating mutations in their KRAS. Because KRAS mutation usually develops during the early phase of pancreatic carcinogenesis and elevated *K*-Ras protein levels have been found inside cancer cells, it has been suggested that the detection of this mutation may provide a diagnostic tool for the early detection of pancreatic cancer.

Radiolabeled antisense oligonucleotides can be used to identify and image the presence of a particular mRNA *in vivo* (5). Some of the major obstacles in the development of a clinically useful radiolabeled antisense probe include nonspecific affinity, ribonuclease destruction of the RNA target, and the lack of a receptor-targeting ligand. Peptide nucleic acids (PNAs) are DNA/RNA mimics in which the nucleobases are attached to a pseudopeptide backbone (6-8). The achiral, uncharged, and flexible PNA peptide backbone permits more stable hybridization to DNA and RNA oligomers with improved sequence selectivity. PNAs are also more stable against nuclease and protease attack, and the uncharged backbone is less likely to react with cellular proteins. However, relatively poor cellular uptake of PNAs requires an additional design strategy such as the addition of a variety of ligands or coupling to different carriers (9). Tian et al. (1) demonstrated that addition of a peptide analog that is specific for a cell surface receptor could be an effective way to increase the cellular uptake of PNAs *in vitro* and *in vivo*. One of the approaches is targeting the IGF1R, which is frequently overexpressed in breast and pancreatic cancer cells. Basu and Wickstrom (10) showed that a 5- to 10-fold uptake increase in cells expressing IGF1Rs *in vitro* could be achieved by solid-phase synthesis of a PNA sequence linked to a cyclized D-amino acid analog of IGF1. Based on this concept, Tian et al. (1, 8) successfully imaged the breast cancer gene CCND1 in experimental human breast cancer xenografts. The authors suggested that the peptide-CCND1 PNA-peptide probe could enter cancer cells that overexpress IGF1R and then hybridize specifically with the oncogene mRNA. Similarly, Chakrabarti et al. (11) synthesized a chelator-*KRAS* PNA-peptide chimera labeled with ^{64}Cu (for PET) and ^{99m}Tc (for SPECT) to target *KRAS* mRNA and image pancreatic cancer in human pancreas cancer xenografts. The mechanism of uptake was tested by IGF1 blocking of breast cancer xenograft imaging with a ^{64}Cu-DO3A-*CCND*1PNA-D(Cys-Ser-Lys-Cys) probe (12). Tian et al. (1, 2) reported successful SPECT imaging of human pancreas cancer xenografts with ^{99m}Tc-4351.

Synthesis

[PubMed]

In PNA, the entire phosphate deoxyribose backbone of DNA/RNA is replaced by a structurally homomorphous polyamide backbone composed of *N*-(2-aminoethyl)glycine units. The PNA-peptide conjugates are generally prepared by fragment condensation (13). This approach requires multiple steps of preparation and purification with significant loss in yield. Basu and Wickstrom (10) used a facile PNA-peptide single-resin synthesis without intermediate conjugation steps. The peptide was first assembled on a solid phase with 9-fluorenylmethoxycarbonyl (Fmoc) coupling. The *t*-Boc–protected PNA monomers were coupled manually. Tian and Wickstrom (14) designed a scheme of a continuous solid-phase synthesis on a single-resin support in a single run to yield, after a single purification, a chimera capable of radionuclide chelation for *in vivo* imaging of gene expression. In this scheme, chelator peptides were extended from the N-terminus of PNA dodecamers, which in turn were extended from the N-termini of disulfide-bridged peptide ligand analogs.

WT4351 is a cyclized peptide-PNA-peptide chimera, $SBTG_2$-DAP-AEEA-GCCAACAGCTCC-AEEA-D(Cys-Ser-Lys-Cys) (1, 11). Briefly, the IGF1 analog D(Cys-Ser-Lys-Cys) was assembled by Fmoc coupling to extend from C to N. The linker Fmoc-aminoethoxyethoxyacetic acid (AEEA) and PNA monomers were then sequentially coupled to the N-terminus of the peptide resin. Finally, the KRAS V12 mutant sequence N-GCCAC-CAGCTCC-C was created, followed by two AEEA spacers, then diaminopropanate (DAP). The chelator moiety SBTG was synthesized and coupled to both amines of deprotected DAP to yield a $SBTG_2DAPN_2S_2$ chelator. The cysteine thiols of D(CSKC) were cyclized on the resin by iodine oxidation, and the chimeras were cleaved, deprotected, and then purified by reverse-phase high-performance liquid chromatography (HPLC). The overall yield of the HPLC-purified WT4351 relative to the initial solid support was ~40%. The mass was calculated to be 4,351.1 Da and measured to be 4,350.5 Da (1, 8).

Radiolabeling was conducted by mixing purified WT4351 with stannous chloride ($SnCl_2$) in 50 mM hydrochloric acid (1, 11). Freshly eluted sodium ^{99m}Tc-pertechnetate from the ^{99}Mo/^{99m}Tc generator in 0.15 M sodium chloride was mixed with a solution of 0.1% Tween 80 in 50 mM sodium phosphate (pH 12). This radionuclide mixture was then added to the WT4351/$SnCl_2$ solution and incubated for 30 min at room temperature. The reaction was neutralized by adding sodium phosphate buffer (pH 4.5). Unchelated ^{99m}Tc and radiolabeled colloids were determined by instant thin-layer chromatography to be 14.1% and 4.4%, respectively. The specific activity of ^{99m}Tc-WT4351 was ~444 MBq (12 mCi)/20 µg or 96.5 kBq (2.6 µCi)/pmol (on the basis of a molecular mass of 4,351.1 Da) WT4351 peptide. The radiochemical yield was not reported.

In Vitro Studies: Testing in Cells and Tissues

[PubMed]

Tian et al. (1) studied the binding of ^{99m}Tc-WT435 by the human pancreatic cancer cell line AsPC1, which expressed a 12th-codon GGT-GAT mutant KRAS. After incubation for 30 min at 37°C, the cell binding (n = 4) was 3,235 ± 316 probes/cell. In comparison, the binding to a non-KRAS probe (^{99m}Tc-WT4185, a CCND1 probe) was 1,151 ± 132 probes/cell. The study suggested that the KRAS specific binding was ~2,000/AsPC1 cell. No cell internalization study was performed.

Animal Studies

Rodents

[PubMed]

Tian et al. (1) administered 18.5 MBq (0.5 mCi) ^{99m}Tc-WT4351 to mice bearing Panc-1 (with KRAS-activating mutation) tumors by i.v. administration for imaging and biodistribution studies. The studies showed rapid and extensive renal excretion of ^{99m}Tc-WT4351. For 24-h distribution studies, a dose of 19.6–34.2 MBq (0.8–0.9 mCi) ^{99m}Tc-WT4351 was administered. The radioactivity levels (n = 4) of ^{99m}Tc-WT4351 in percentage

injected dose per gram (% ID/g) at 4 h were 0.22 ± 0.03 (tumor), 0.27 ± 0.07 (blood), 5.19 ± 1.72 (liver), 90.18 ± 7.22 (kidney), 1.07 ± 0.26 (spleen), and 0.19 ± 0.03 (muscle). The tumor/blood and tumor/muscle ratios were 0.83 ± 0.19 and 1.14 ± 0.20, respectively. At 24 h, the radioactivity levels (n = 5) were 0.14 ± 0.05 (tumor), 0.06 ± 0.01 (blood), 5.68 ± 0.46 (liver), 65.96 ± 5.76 (kidney), 1.00 ± 0.09 (spleen), and 0.07 ± 0.03 (muscle). The tumor/blood and tumor/muscle ratios were 2.37 ± 0.84 and 2.14 ± 0.74, respectively.

Gamma imaging of 18.5 MBq (0.5 mCi) ^{99m}Tc-WT4351 in mice bearing Panc-1 tumors showed tumor/contralateral muscle image intensity ratios of 5.4 at 4 h and 2.7 at 24 h (1, 11). Tian et al. (2) reported a similar strong signal at 4 h and a weaker signal at 24 h when imaging ^{99m}Tc-WT4351 in mice bearing AsPC1 pancreatic tumors. No specific blocking study was conducted.

Other Non-Primate Mammals

[PubMed]

No publication is currently available.

Non-Human Primates

[PubMed]

No publication is currently available.

Human Studies

[PubMed]

No publication is currently available.

NIH Support

NCI grant CA42960, NCI contract CO27175, NIH grant HL59769, CA109231.

References

1. Tian X., Chakrabarti A., Amirkhanov N.V., Aruva M.R., Zhang K., Mathew B., Cardi C., Qin W., Sauter E.R., Thakur M.L., Wickstrom E. External imaging of CCND1, MYC, and KRAS oncogene mRNAs with tumor-targeted radionuclide-PNA-peptide chimeras. Ann N Y Acad Sci. 2005; **1059** :106–44. PubMed PMID: 16382049.
2. Tian X., Chakrabarti A., Amirkhanov N., Aruva M.R., Zhang K., Cardi C.A., Lai S., Thakur M.L., Wickstrom E. Receptor-mediated internalization of chelator-PNA-peptide hybridization probes for radioimaging or magnetic resonance imaging of oncogene mRNAs in tumours. Biochem Soc Trans. 2007; **35** (Pt 1):72–6. PubMed PMID: 17233604.
3. Mancuso A., Calabro F., Sternberg C.N. Current therapies and advances in the treatment of pancreatic cancer. Crit Rev Oncol Hematol. 2006; **58** (3):231–41. PubMed PMID: 16725343.
4. Talar-Wojnarowska R., Malecka-Panas E. Molecular pathogenesis of pancreatic adenocarcinoma: potential clinical implications. Med Sci Monit. 2006; **12** (9):RA186–93. PubMed PMID: 16940943.
5. Gauchez A.S. A. Du Moulinet D'Hardemare, J. Lunardi, J.P. Vuillez, and D. Fagret, *Potential use of radiolabeled antisense oligonucleotides in oncology.* Anticancer Res. 1999; **19** (6B):4989–97. PubMed PMID: 10697501.
6. Good L., Nielsen P.E. Progress in developing PNA as a gene-targeted drug. Antisense Nucleic Acid Drug Dev. 1997; **7** (4):431–7. PubMed PMID: 9303195.

7. Ray A., Norden B. Peptide nucleic acid (PNA): its medical and biotechnical applications and promise for the future. Faseb J. 2000; **14** (9):1041–60. PubMed PMID: 10834926.
8. Tian X., Aruva M.R., Qin W., Zhu W., Duffy K.T., Sauter E.R., Thakur M.L., Wickstrom E. External imaging of CCND1 cancer gene activity in experimental human breast cancer xenografts with 99mTc-peptide-peptide nucleic acid-peptide chimeras. J Nucl Med. 2004; **45** (12):2070–82. PubMed PMID: 15585484.
9. Soomets U., Hallbrink M., Langel U. Antisense properties of peptide nucleic acids. Front Biosci. 1999; **4** :D782–6. PubMed PMID: 10568787.
10. Basu S., Wickstrom E. Synthesis and characterization of a peptide nucleic acid conjugated to a D-peptide analog of insulin-like growth factor 1 for increased cellular uptake. Bioconjug Chem. 1997; **8** (4):481–8. PubMed PMID: 9258444.
11. Chakrabarti A., Aruva M.R., Sajankila S.P., Thakur M.L., Wickstrom E. Synthesis of novel peptide nucleic acid-peptide chimera for non-invasive imaging of cancer. Nucleosides Nucleotides Nucleic Acids. 2005; **24** (5-7):409–14. PubMed PMID: 16247960.
12. Tian X., Aruva M.R., Zhang K., Shanthly N., Cardi C.A., Thakur M.L., Wickstrom E. PET Imaging of CCND1 mRNA in Human MCF7 Estrogen Receptor Positive Breast Cancer Xenografts with Oncogene-Specific [64Cu]Chelator-Peptide Nucleic Acid-IGF1 Analog Radiohybridization Probes. J Nucl Med. 2007; **48** (10):1699–1707. PubMed PMID: 17909257.
13. Tung C.H., Stein S. Preparation and applications of peptide-oligonucleotide conjugates. Bioconjug Chem. 2000; **11** (5):605–18. PubMed PMID: 10995203.
14. Tian X., Wickstrom E. Continuous solid-phase synthesis and disulfide cyclization of peptide-PNA-peptide chimeras. Org Lett. 2002; **4** (23):4013–6. PubMed PMID: 12423074.